CHARACTERIZATION OF TITANIUM NITRIDES FORMED DURING STEEL SOLIDIFICATION*

Constantino Capurro[1]
Carlos Cicutti[2]

Abstract
For certain applications, coarse titanium nitride (TiN) precipitates can be deleterious for the final properties of the material. Hence, in order to better understand the mechanisms involved in the generation of these precipitates, a thorough characterization of the particles observed in steels with different titanium and nitrogen content was carried out. Samples from liquid steel (tundish), continuous casting billets and final product were evaluated using an Automatic Particle Analyzer (APA) coupled to a Scanning Electronic Microscope (SEM). The location, frequency, size distribution and composition of the different particles observed were assessed. While only few TiN precipitates were observed in liquid steel samples, the density of this type of particle significantly increased in the continuous casting billets samples. Particles ranging from 1 to 10 µm were mainly found in the interdendritic zones of the as-cast structure. The density of TiN particles observed in these samples did not change after re-heating and rolling operations. A model to predict TiN precipitation during solidification was developed. A reasonable agreement was found between model results and measured data. Results of this analysis confirmed that the precipitated fraction of TiN increases as the product of steel Ti and N contents rises.
Keywords: Titanium Nitrides, Solidification, Continuous Casting, Model.

[1] *Materials Engineer, Senior Researcher R&D Steelmaking Department,* Tenaris Siderca R&D Center, J. Simini 250 (2804) Campana, Argentina, E-mail: **ccapurro@tenaris.com**
[2] *PhD in Materials Science, R&D Steelmaking Department Manager,* Tenaris Siderca R&D Center, J. Simini 250 (2804) Campana, Argentina, E-mail: **ccicutti@tenaris.com**

1 INTRODUCTION

Titanium is normally added to steels for several purposes [1,2]. In some cases, the addition is performed to inhibit the formation of boron nitrides that impair steel hardenability [3,4]. In others, Ti addition has the objective of limiting grain growth during heating before rolling [5], or in the Heat Affected Zone (HAZ) of welded structures [6]. Titanium also plays an important role in the mechanical properties of the final product [7]. In Interstitial Free (IF) steels, the formation of titanium carbides and nitrides improves the drawing capacity, minimizing the ageing of the material [8]. It has also been suggested that Ti could help in the modification of product microstructure, because the oxides that are formed promote acicular ferrite precipitation [9]. Also the nitrides could be active in microstructure modification [9]. Titanium addition in Nb alloyed steels has proven to be effective to improve ductility of continuous casting products. This is because precipitation of niobium rich fine precipitates is minimized [10,11]. Nevertheless, the effect of Ti on high temperature ductility is still under debate [12,13]. Some recent studies have shown that titanium could refine austenitic grain size in the cast structure [14,15].

In any of the aforementioned applications, Ti addition can promote titanium nitride (TiN) precipitation during steel solidification. These TiN particles formed from liquid phase have cuboidal shape and relatively big sizes (1-20 µm), compared with those formed in solid state during subsequent process stages, which sizes may range between 10-100 nm. While the later have specific metallurgical functions, such as control of grain growth, the former can deteriorate material toughness, by promoting cleavage crack propagation [6,16-19]. In certain applications, like steels for ball bearings, these coarse precipitates can also impair fatigue properties [20].

In the present paper, a thorough characterization of the precipitates found in medium carbon steels with different Ti and N contents was performed. Samples from different stages of the process (liquid steel, as-cast billets and final product) were obtained for analysis. In addition, a model to predict the formation of these precipitates during steel solidification was developed.

2 MATERIAL AND METHODS

2.1 Analyzed samples

Samples were obtained from seamless pipes of eight different heats of medium carbon steels, with different titanium and nitrogen contents, see Table 1. These pipes were rolled from round billets produced following the route: Electric Arc Furnace – Ladle Furnace – Continuous Casting. In one of the analyzed heats (C003), samples from three different pipes were obtained to verify consistency in the obtained results. To complement the analysis, liquid steel samples from tundish and as-cast samples from the continuous casting billets were also obtained in some of the studied heats, see Table 1. In all the samples, precipitates were characterized applying the technique described in the following section.

Pipe samples were sectioned longitudinally, as shown in Figure 1 a). To assess possible differences in through thickness direction, the analyzed zone was divided into 10 smaller equal zones. Total scanned area was about 90 mm^2. In the as-cast

material, 25 mm x 25 mm samples were prepared to characterize one billet radius, scanning also 90 mm^2 per sample, see Figure 1 b). As-cast microstructure was revealed etching the samples with different reagents (Nital, Oberhoffer). In the sample taken from the center of the billet (sample C, Figure 1 b)) additional studies were carried out to characterize central porosity. Finally, in lollypop samples taken from tundish, one of the faces was polished and an area of 90 mm^2 was also scanned to characterize the particles found.

Table 1. Ti and N content in the analyzed cases

Heat	Ti (%)	N (%)	Ti/N (-)	Ti*N (10^{-4} $\%^2$)	Sample
C001	0.022	0.0064	3.45	1.408	Pipe
C002	0.025	0.0081	3.09	2.025	Tundish/Billet/Pipe
C003	0.023	0.0044	5.23	1.012	Tundish/Billet/Pipe
C004	0.020	0.0063	3.16	1.264	Tundish/Billet/Pipe
C005	0.012	0.0045	2.67	0.540	Pipe
C006	0.011	0.0055	2.00	0.605	Pipe
C007	0.012	0.0046	2.61	0.552	Pipe
C008	0.019	0.0048	3.96	0.912	Pipe

Base composition: 0.25 %C, 0.35 % Mn, 0.21 %Si, 1 % Cr, 0.7 % Mo, 0.025 % Nb, 0.03 %, Al, 15 ppm S, 12 ppm Ca

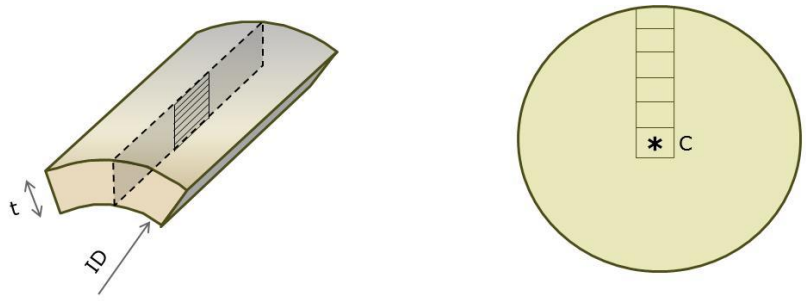

Figure 1. Samples for analysis.
(a) Seamless pipes, (b) Continuous Casting Bars.

2.2 Characterization of the precipitates

The obtained samples were polished and analyzed by means of a Scanning Electronic Microscope (SEM) equipped with Energy Dispersive Spectroscopy (EDS). Inclusion and precipitates population was evaluated using an Automatic Particle Analyzer (APA) software incorporated to the SEM following a procedure described elsewhere [21,22]. In order to identify the nitrides with better precision, the minimum particle size was lowered to 1.4 µm (instead of the 2.7 µm used in the original procedure). Most of the precipitates normally look darker than steel matrix with the SEM backscattered electrons detector, which allows an easy identification by the APA. However, as the analyzed steels contain niobium in their composition (Table 1), Nb precipitates would appear brighter than the steel matrix. Hence, samples were analyzed twice, setting the APA brightness threshold to assess particles darker and brighter than the steel matrix. Anyway, as it is shown in the following section, the number of bright precipitates in the analyzed samples was relatively low, so the analysis was mainly focused in the dark particles, observed with the usual procedure.

3 RESULTS AND DISCUSSION

3.1 Typically observed particles

Preliminary analysis revealed the presence of three types of particles within the steel matrix: oxides, sulfides and nitrides (or carbonitrides), together with their possible combinations. As an example, Figure 2 shows the distribution between the different families for one of the analyzed samples. It is clear that nitrides are the predominant particles, followed by oxy-sulfides, oxides and sulfides. The same pattern was observed in most of the samples. Dark nitrides mainly contain Ti, with small amounts of Nb, as shown in Figure 3 a). Their shape is cuboidal, with sharp edges, as reported in the literature [23]. In some cases, these TiN particles are associated to oxide inclusions that remain in the liquid steel after the secondary metallurgy stages. Brighter particles have high niobium content with traces of Ti, see Figure 3 b). Nevertheless, as mentioned before, the number of Nb-rich particles was very low compared to Ti-rich precipitates.

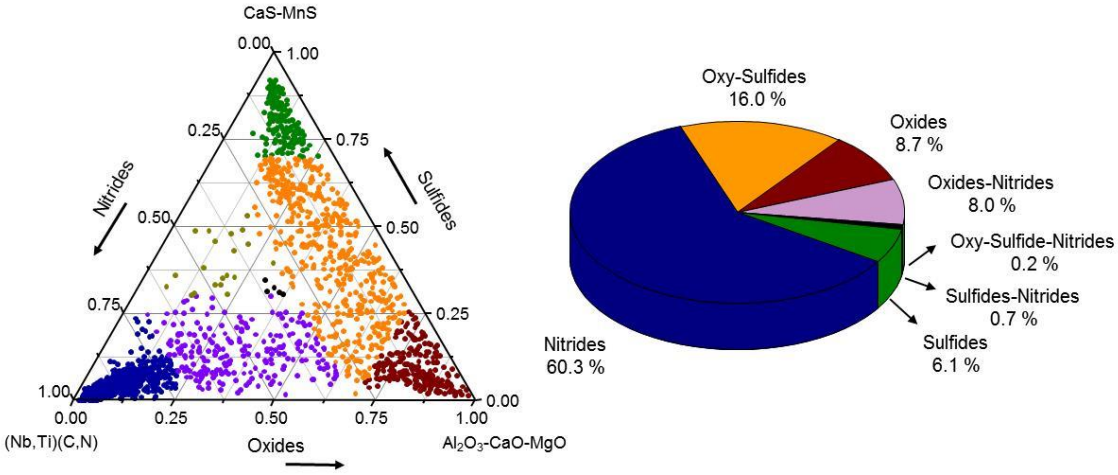

Figure 2. Example of the type of particles observed in one of the analyzed samples.

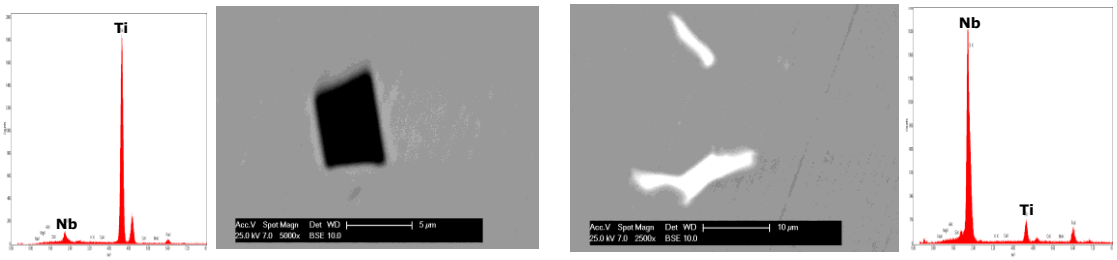

Figure 3. Nitrides and/or carbonitrides typically observed in the analyzed samples. a) Ti-rich precipitates, b) Nb-rich precipitates.

3.2 Particles density in the analyzed samples

Particle densities measured in all the final product samples are summarized in Figure 4 a). For the sake of clarity, only those families with larger amounts of particles are shown: oxides, sulfides, oxy-sulfides and nitrides. Although there are some variations

from one heat to another, a high proportion of nitrides are detected in most of the analyzed cases. Good consistency of results was also verified in the three samples obtained from the same heat (C003).

In order to evaluate the effect of processing steps on the density of particles, samples taken at liquid steel, after casting and in the final product were evaluated in three of the studied heats (Table 1). Results of this analysis are presented in Figure 4 b). For all the evaluated heats, the particle density measured in final product is similar to that obtained in as-cast samples. The same result is observed for the different particles families considered, suggesting that hot rolling and heat treatment stages do not introduce major modifications in these precipitates. It means that no dissolution nor coalescence of particles occurs during the thermomechanical treatment. This is in agreement with previous studies that reported that “coarse” TiN precipitates formed during solidification are not altered by subsequent process treatments [18].

However, in the case of liquid steel samples, a different pattern is observed. While the densities of oxides, oxy-sulfides and sulfides are similar to those obtained in as-cast and final product samples, the amount of nitrides is significantly lower. This result suggests that these particles precipitate during steel solidification. With the aim of verifying this observation, further analysis was performed and is discussed in the next section.

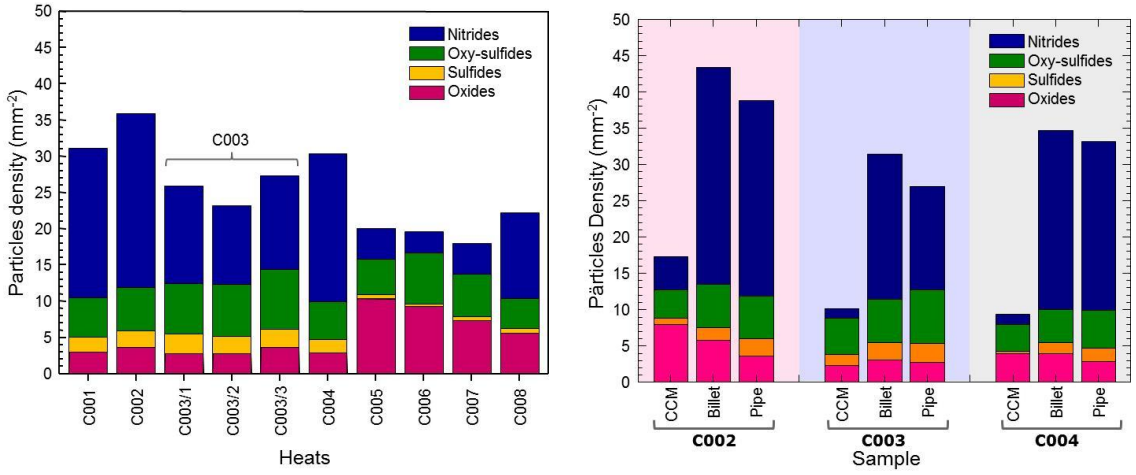

a) **b)**

Figure 4. Particles density measured in the different samples.
a) Individual values for all the analyzed pipe samples,
b) Comparison of results obtained in liquid steel, as-cast and final product samples.

3.3 Location of the particles in the as-cast structure

Analysis of the as-cast material revealed that TiN particles were mainly located in the segregated areas of the dendritic structure. As an example, Figure 5 a) shows the segregation pattern observed after the sample was etched (Oberhoffer). The dark areas indicate the segregation pattern developed by the dendritic growth. Titanium rich particles are located preferentially in these darker zones, suggesting that they are precipitated at the end of the solidification process. In addition, the analysis of the sample taken from the center of the as-cast billet (sample C in Figure 1) showed the precipitation of these particles at the solidification front. Shrinkage of the steel in the

final stages of solidification removes interdendritic liquid exposing the dendrites. Figure 5 b) shows one of these regions, were several TiN particles can be observed.

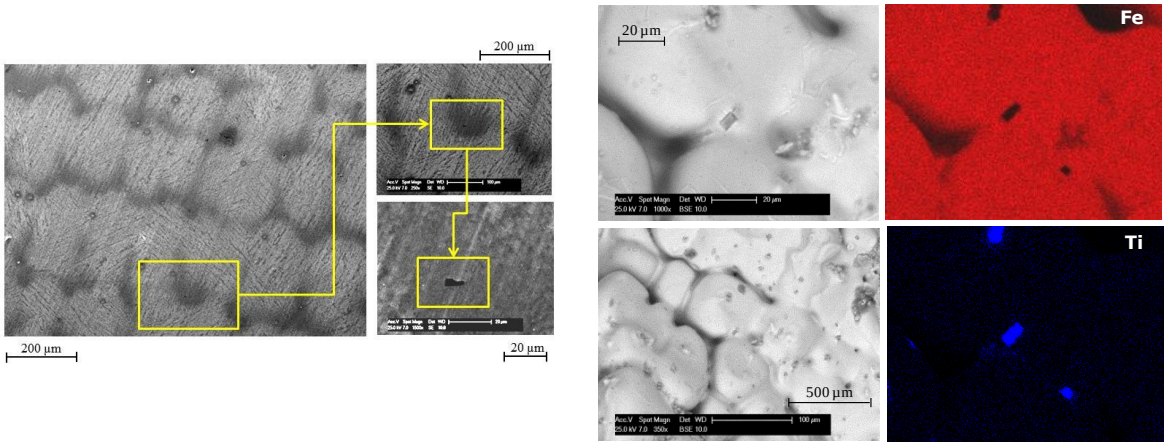

Figure 5. Location of TiN precipitates in the as-cast structure.
a) In the segregated zone of the solidification structure (Oberhoffer), b) TiN particles precipitated at the surface of the dendritic front (Sample taken from center of the billet).

3.4 Precipitated fraction

By means of the APA measurements carried out with the SEM, it is possible to determine not only the density of particles but also the fraction of area occupied by them. Assuming that the volumetric fraction is equal to the measured area fraction [24], the amount of TiN precipitates ($wt\%$) can be calculated as indicated by Equation (1):

$$m^{TiN}(\%) = 0.01 \cdot A_A^{TiN} \cdot \rho_{TiN}/\rho_{Fe} \quad (1)$$

where ρ_{Fe} and ρ_{TiN} are iron and TiN densities respectively (7800 and 5420 kg/m^3 [25]).

In order to evaluate the effect of steel composition on the amount of coarse titanium nitrides precipitated during solidification, different studies were performed. Figure 6 shows the effect of the product Ti•N and the ratio Ti/N on the mass fraction of precipitates. These results indicate that the amount of TiN precipitates is more affected by the product of titanium and nitrogen concentration than by their ratio, which is in agreement with the conclusions obtained by other researchers [3].

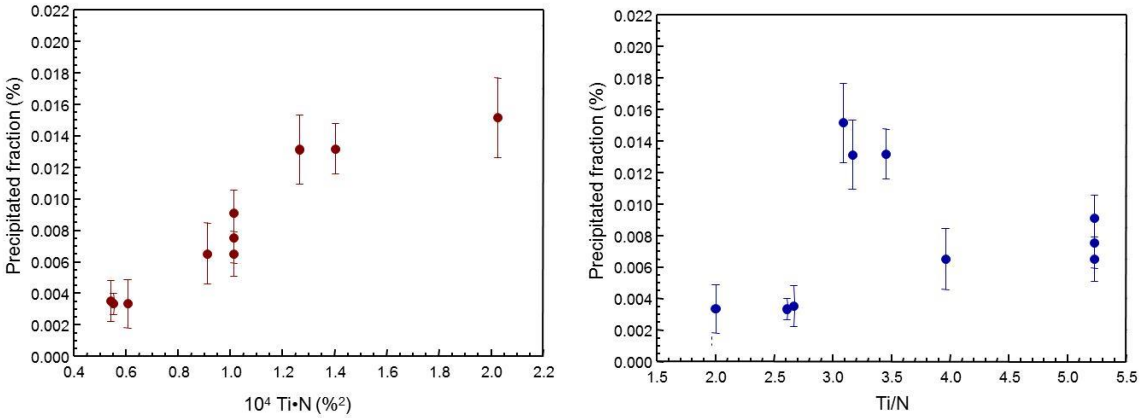

Figure 6. Influence of Ti and N content on the precipitated fraction of TiN.
a) Effect of the product Ti•N b) Effect of Ti/N ratio.

3.5 Precipitates size

In most of the analyzed samples, the average size of the different particles found was around 3-5 μm. The typical size distribution observed for titanium nitrides is shown in Figure 7 a). This distribution can be adequately described with a log-normal type function, similar to the one applied for the size distribution of "fine" TiN particles (1–10 nm) that precipitates in solid state [26], Equation [2] and Figure 7 b):

$$p = \frac{1}{d \cdot \sigma \cdot \sqrt{2 \cdot \pi}} \cdot exp\left[-\frac{(lnd-\mu)^2}{2 \cdot \sigma^2}\right] \quad (2)$$

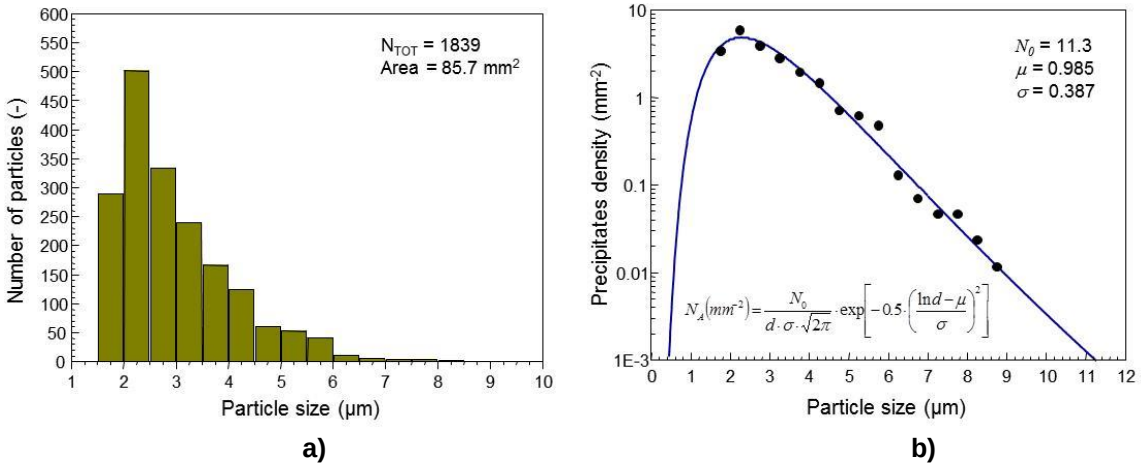

Figure 7. Size of observed TiN precipitates.
a) Typical size distribution, b) Fitting of a log-normal distribution.

As shown in Figure 8 a), the average size of TiN particles tends to increase with the distance to product surface. However, in the case of oxides, the particle size is not affected by their position in the product, Figure 8 b). This behavior can be explained by the fact that oxides are already present in the liquid steel before solidification starts but titanium nitrides precipitate and grow in the interdendritic liquid. Hence, longer local solidification times will promote larger precipitates. As local solidification time increases with the distance to steel surface, the average size of TiN particles

also tends to increase. A similar effect has been reported for other particles that precipitate in the interdendritic liquid, such as manganese sulfides [27].

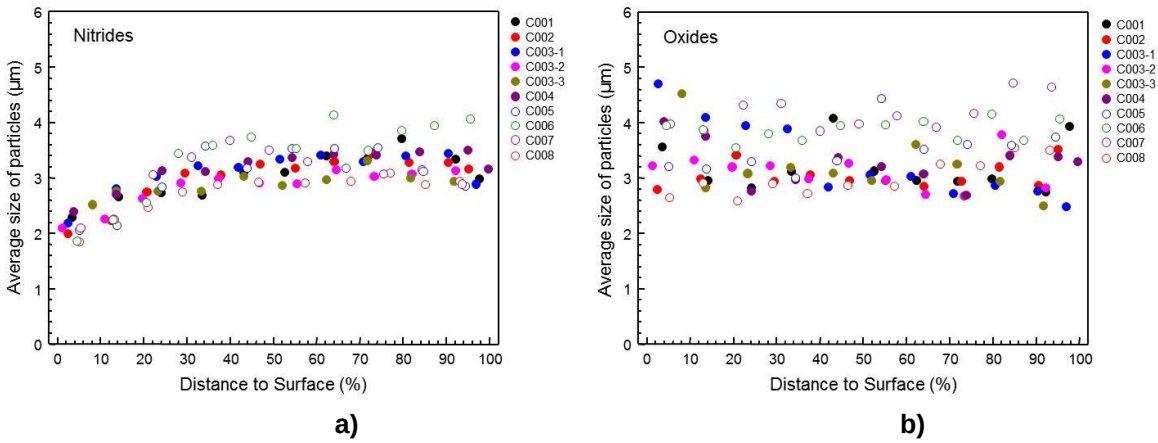

Figure 8. Variation of particles size with the distance to final product surface. a) Titanium nitrides, b) Oxides.

4. MODEL TO PREDICT TiN PECIPITATION DURING SOLIDIFICATION

4.1 Theoretical background

A microsegregation model previously developed [28,29] that calculates how the concentration of the different alloying elements vary in the interdendritic liquid as solidification evolves was used as starting point. The original procedure takes into account the peritectic reaction phase change, δ/γ, and it is able to determine the temperature evolution during solidification. This model was adapted to assess the precipitation of TiN during solidification. This happens when the concentration of Ti and N in the liquid overcome the solubility product. The formation reaction of titanium nitride can be expressed as:

$$[Ti] + [N] = TiN_{(s)} \quad K_{TiN} = \frac{a_{TiN}}{f_{Ti}[Ti] \cdot f_N[N]} \tag{3}$$

where activity coefficients f_{Ti} and f_N are calculated by means of the Wagner formalism for diluted solutions with the corresponding interaction parameters [30], whereas the reaction equilibrium constant (K_{TiN}) is a temperature dependent function [10]. The higher concentration of these alloying elements and the lower temperatures in the last stages of solidification promote the precipitation of TiN in the interdendritic liquid.

4.2 Model results

For the different analyzed heats (Table 1), model results were compared with SEM measurements performed on pipe samples. Results are presented in Figure 9 a), where a reasonable agreement between measured and calculated data is observed. As mentioned before, the measured fraction of TiN precipitates increases with the product of Ti and N concentrations in bulk steel (Figure 6 b). Simulations performed with the developed model also predict a similar trend, Figure 9 b.

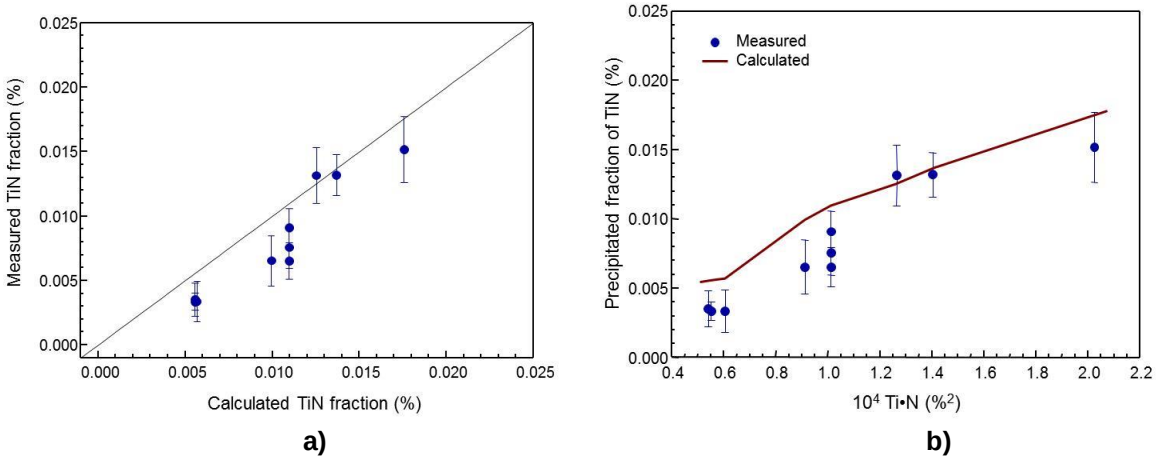

Figure 9. Results of model calculations
a) Comparison between measured and calculated TiN precipitated fraction,
b) Effect of the product Ti•N. on the fraction of precipitates.

5 CONCLUSIONS

An intensive characterization of the precipitates observed in medium carbon steels with different titanium and nitrogen contents was carried out. In addition to the oxides and sulfides normally found in these steels, a high number of Ti rich precipitates with sizes ranging from 1 to 10 µm were detected in the final product.

The density of these particles in the final product was similar to that measured in the as-cast material, indicating that hot rolling and heat treatment stages do not introduce major modifications. However, the amount of TiN particles measured in liquid steel samples was significantly lower, which suggests that they precipitate during steel solidification.

Further analysis of as-cast material showed that TiN particles are mainly located in the interdendritic regions of the microstructure, which confirms that precipitation principally takes place in the final stages of steel solidification. Moreover, it was also observed that the average size of these precipitates tends to increase with the distance to product surface, which can be explained by the fact that the local solidification time also increases with the distance to the surface.

Processing the information collected during SEM analysis it is possible to estimate the mass fraction of precipitated TiN. For the group of evaluated steels, this analysis revealed that the fraction of TiN increases with the product of titanium and nitrogen concentration in bulk steel.

Finally, a microsegregation model to predict the formation of TiN particles during steel solidification was implemented. Model results showed a reasonable agreement with the amount of TiN measured in the final product samples.

REFERENCES

1 Pickering F. Overview of Titanium microalloyed steels. IoM Titanium Technology in Microalloyed Steels. 1994: 10-43.
2 Paules J., Marshall J. An overview of the uses of Titanium in the US industry. In: ISS-AIME 35th Mechanical Working and Steel Processing Conference; Pittsburgh, Pa, USA. Pittsburgh: ISS-AIME; 1994, p. 445-452.
3 Shen Y., Hansen S. Effect of the Ti/N ratio on the hardenability and mechanical properties of a quenched and tempered C-Mn-B steel. Metallurgical Transactions A. 1997; 28A: 2027-2035.
4 Olivo P., Sosa D., Echaniz G., Patané M. Influence of Ti/N ratio on the heat treatment set-up for Boron-Titanium Carbon-Manganese steels for seamless Oil Country Tubular Goods. 3rd IAS Conference on uses of Steel; 2006, San Nicolás, Argentina. San Nicolás: IAS; 2006. p. 105-112.
5 Medina S., Chapa M., Valles P., Ouispe A., Vega M. Influence of Ti and N contents on austenite grain control and precipitate size in structural steels. ISIJ International. 1999; 39(9): 930-936.
6 Zhang L., Davis C., Strangwood M. Effect of TiN particles and microstructure on fracture toughness in simulated heat affected zones of a structural steel. Metallurgical and Materials Transactions A. 1999; 30A: 2089-2096.
7 Kunishige K., Nagao N. Strengthening and toughening of hot-direct-rolled steels by addition of a small amount of Titanium. ISIJ International. 1989; 29(11): 940-946.
8 Takechi H. Metallurgical aspects on Interstitial Free sheet steel from industrial viewpoints. ISIJ International. 1994; 34(1): 1-8.
9 Sarma D., Karasev V., Jönsson P. On the role of non-metallic inclusions in the nucleation of acicular ferrite in steels. ISIJ International. 2009; 49(7); 1063-1074.
10 Turkdogan E. Causes and effects of nitride and carbonitride precipitation during continuous casting. Iron and Steelmaker. 1989: 61-75.
11 Patrick B., Ludlow V. Development of casting practices to minimize transverse cracking in microalloyed steels. Revue de Metallurgie CIT. 1994: 1081-1089.
12 Abushosha R., Cominelli O., Mintz B. Influence of Ti on hot ductility of C-Mn-Al steels. Materials Science and Technology. 1999; 15: 278-286.
13 Cicutti C., Martín M., Alzari S., Di Gresia G. Analysis of the source of transverse cracks in continuously cast slabs of titanium bearing, medium carbon steels. 17th IAS Steelmaking Conference; 2009, Rosario, Argentina. Rosario: IAS; 2009, 186-195.
14 Ohno M., Matsuura K. Refinement of as-cast austenite microstructure in S45C steel by Titanium addition. ISIJ International. 2008; 48(10): 1373-1379.
15 Sasaki M., Matsuura K., Ohsasa K., Ohno M. Refinement of as-cast austenite grain in carbon steel by addition of Titanium. ISIJ International. 2009; 49(9): 1362-1366.
16 Yan W., Shan Y., Yang K. Effect of TiN inclusions on the impact toughness of Low-Carbon Microalloyed Steels. Metallurgical and Materials Transactions A. 2006; 37A: 2147-2158.
17 Yan W., Shan Y., Yang K. Influence of TiN inclusions on the cleavage fracture behavior of Low-Carbon Microalloyed Steels. Metallurgical and Materials Transactions A. 2007; 38A: 1211-1222.
18 Jubleanu A. Carbo-nitride precipitation and its effects on matrix transformations in high strength high toughness 300M steel. Ms Thesis. Birmingham: University of Birmingham; 2009.
19 Balart M., Davies C., Strangwood M. Observations of cleavage initiation at (Ti,V)(C,N) particles of heterogeneous composition in microalloyed steels. Scripta Materialia. 2004; 50: 371-375.
20 Monmot J., Heritier B., Cogne J. Relationship of melting practice, inclusion type and size with fatigue resistance of bearing steels. Effect of Steel Manufacturing Process on the Quality of Bearing Steels, ASTM STP 987. 1988: 149-165.

21 Capurro C., Cerrutti G., Cicutti C. Study of the generation and modification of spinel type inclusions during secondary metallurgy and casting stages. 19th IAS Steel Conference; 2013, Rosario, Argentina. Rosario: IAS, 2013, 332-341.
22 Capurro C., Cicutti C., Carranza A., Escorza E. Efecto de la composición de las inclusiones en la colabilidad de los aceros resulfurados. 16th IAS Steelmaking Conference; 2007, San Nicolás, Argentina. San Nicolás: IAS, 2007, 433-440.
23 Du J., Strangwood M., Davis C. Effect of TiN particles and grain size on the Charpy impact transition temperature in steels. Journal of Materials Science and Technology. 2012; 28(10): 878-888.
24 Russ J., Dehoff R. Practical Stereology, 2nd Edition, Plenum Press; 1999.
25 Gladman T. The physical metallurgy of microalloyed steels. The Institute of Metals; 1997; p. 207.
26 Moon J., Lee C., Uhm S., Lee J. Coarsening kinetics of TiN particle in a low alloyed steel in weld HAZ: considering critical particle size. Acta Materialia. 2006; 54: 1053-1061.
27 Oikawa K., Ishida K., Nishizawa T. Effect of Titanium addition on the formation and distribution of MnS inclusions in steel during solidification. ISIJ International. 1997; 37(4): 332-338.
28 Cicutti C., Boeri R. Desarrollo de un modelo para calcular la distribución de soluto durante la solidificación de aceros de baja aleación. 13th IAS Steelmaking Seminar; 2001, Buenos Aires, Argentina. Buenos Aires: IAS, 2001, 711-718.
29 Cicutti C., Boeri R. Analysis of solute distribution during the solidification of low alloyed steels. Steel Research International. 2006; 77(3): 194-201.
30 Sigworth G., Elliot J. The thermodynamics of liquid dilute iron alloys. Metal Science. 1974; 8(9): 298-310.